© 2017 IJSRST | Volume 3 | Issue 7 | Print ISSN: 2395-6011 | Online ISSN: 2395-602X
Themed Section: Science and Technology

Electronic structural UV-Vis analysis of 7, 8-dihydroxy - 4 - Phenyl Coumarin Monohydrate reinforced by DFT approach

C. N. Dipunadas
Department of Physics, Christian College, Kattakada, Kerala, India

ABSTRACT

In present research work, coalesce of experimental and theoretical study on optimized molecular structure of 7, 8-dihydroxy-4-Phenyl Coumarin Monohydrate (DHPC) have been reported. Downshifting frequencies of O-H vibrations due to intra-molecular O-H…O hydrogen bonding as well as intramolecular interactions with solvent molecule confirmed by spectral analysis were resolved by natural bond orbital analysis. Broad, intense bands were observed for different solvents in UV-Vis peak absorption wavelengths. Frontier orbital energy gap (EHOMO–ELUMO), a critical parameter in determining charge transfer properties and bioactive efficiency is found to be -3.96 eV.

Keywords : DHPC, UV-Vis, HOMO-LUMO, NBO

I. INTRODUCTION

Coumarin, the cyclic chemical compounds bearing an unsaturated six membered ring containing one oxygen atom and a ketone functional group, that possess conjugated system with rich electron and good charge transfer from electron-rich substituents[1,2]. Coumarin derivatives act as skin and health benefit agent used to fabricate functional molecules in pharmacological area. In recent era, coumarins attracted special interest as medicinal drug candidate owing to their potential biological activities such as antibacterial, anti-inflammatory, antioxidant, anti-tumour activity [3-6] and also identified as protease and integrase inhibitors[7,8]. Veselinović et al. [9] reported 4-phenyl hydroxycoumarins as good molecular models for potential antibacterial agents and can act as free radical scavengers. Koketsu et al. [10] synthesized and reported various coumarin derivatives as effective agents for relieving inflammation symptoms in the body.

7,8-dihydroxy-4phenyl coumarin monohydrate (DHPC) belongs to neoflavonoid family having C3-C4 double bond and 4-phenyl chromene backbone and no literature survey reveals the vibrational spectroscopic studies as well as density functional theoretical studies of title compound. Spectroscopic techniques along with density functional theory (DFT) computations have achieved substantial interest in determining molecular structural elucidation, physical and chemical properties leading to the bioactive nature of the compound. This article highlights the hydrogen bonding interactions confirmed by calculated results supporting the experimental results revealing electronic properties by ultraviolet visible (UV-Vis) analysis.

II. Experimental and Computational Details

Powder form of 7,8dihydroxy4-phenylcoumarin monohydrate was purchased from Sigma Aldrich Company with a stated purity greater than 98% used as such without any further purification. UV absorption spectra of DHPC were examined in the range 200-400 nm based on ASTME 169-04 using Varian, CARY 100 BIO UV-Visible Spectrophotometer in ethanol, methanol and DMSO solutions.

Geometry optimization and vibrational wavenumber were performed using Becke-3-Lee-Yang-Parr (B3LYP) gradient correlation functional with 6-311++G(d,p) the basis set [11-15] using Gaussian 09W program package developed by Frisch and co-workers [16]. Natural bond orbital (NBO) [17] calculation was performed using NBO 3.1 program as implemented in the Gaussian 09W package performed in gas phase. NBO analysis summarizes hybridization of atomic lone pairs and of the atoms involved in bond orbitals. Mixing of the donor and acceptor orbitals can be treated with second-order

perturbation theory analysis to expound the intramolecular bonding, rehybridization and delocalization of electron density within the molecule which was performed at the DFT-B3LYP/6-311++G(d,p) [18,19] level of theory. By considering solvent effect, energies of highest occupied molecular orbital (HOMO) and the lowest unoccupied molecular orbital (LUMO) were computed. Time-dependent density functional theory (TD-DFT) calculations were carried out in ethanol solvent in order to predict electronic excitation energies while UV-vis absorption spectrum of DHPC measured ethanol solvent was recorded.

III. RESULTS AND DISCUSSION

3.1 Molecular geometry

Structural optimization at ground state level of DHPC have been performed using B3LYP/6-311++G(d,p) basis set is shown in figure 1. Bond length depends on the bond order, orbital hybridization and resonance or delocalization of π-electrons of a molecule. C=O bond length of Coumarin derivatives expected to lie in the range of 1.183-1.210 Å is observed as C_2-O_{11}=1.21Å with force constant (11.09 m dyne/Å). Ring C-O bond length in α-pyrone ring is expected to lie in the region 1.34-1.36Å, but due to the existence of strong repulsive interaction between adjacent oxygen lone electron pairs and carbonyl oxygen, alkyl oxygen bond length O_1-C_6=1.36Å become less than acyl oxygen bond length O_1-C_2=1.38Å. Since hydroxyl is electron withdrawing through sigma bonds (-I effect) and electron donating through pi bonds carbon atoms attached to hydroxyl group have bond lengths C_7-O_{17}=C_8-O_{15}=1.35Å which agrees with the values of both experimental and reported compound [20]. Aromatic C-C bond length expected to occur in the range of 1.37-1.40Å [21] and bond length across rings almost agrees but elongation happens (C_2-C_3=1.44/1.42 Å; C_4-C_5=1.45/1.44Å) as single bonds are involved in the electron delocalization due to resonance as well as hyperconjugation. Bond lengths and bond angles of Ring A vary because of the electron cloud surrounding each atom repel each other (steric effect) leading to destabilization.

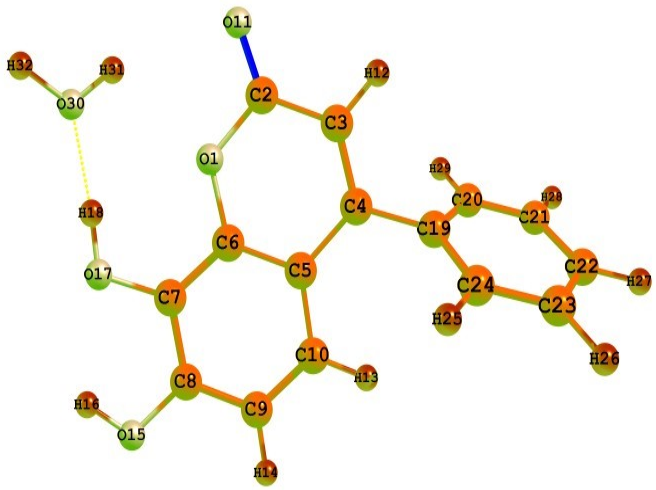

Figure 1. Optimized Molecular structure of DHPC

Carbonyl centre in esters gives rise to C–C–O and O–C–O (120°) angles but in DHPC, bond angles gets distorted and deviates due to resonance effect of carbon atoms having (sp) hybridization. Deviation of bond angles is due to partial double bond character on account of the conjugation of unshared electron pair of oxygen C_7-O_{17}-H_{18}= (113.83/112.99)° and C_8-O_{15}-H_{16}= (107.96/114.58)° within the coumarin moiety. Decrease in bond angle (C_6-C_7-C_8=118/117°) is due to the presence of electron withdrawing effect of hydroxyl group through sigma bonds at the 7-position. In the title compound, coumarin moiety is planar with phenyl ring A attached to C_4 atom but phenyl ring is oriented away within ≈2° out of coumarin plane Dihedral angle between ring B and α-pyrone ring C is -55.1° and that between ring A and ring C in the coumarin skeleton is 178.9°.

3.2 Natural bond orbital and natural hybrid orbital (NHO) directionality analysis

Higher electronegativity reflects larger polarization coefficients across acyl and alkyl oxygen atoms and the linear combination of its constituent natural hybrid orbitals are

$$\sigma O1C2 = 0.8389(sp^{2.17})_O + 0.5442(sp^{3.13})_C ;$$
$$\sigma O1C6 = 0.8260(sp^{1.85})_O + 0.5442(sp^{3.26})_C$$

Donation of an out-of-plane π lone pair $LP_2O1 \rightarrow \pi^*C2$-O11 has higher stabilization energy 34.55 kcal/mol than the donation of in-plane σ lone pair $LP_1O1 \rightarrow \sigma^*C2$-O11(2.39kcal/mol). Hybrid directionality and bond

bending analysis of NHOs provide hints of angular deformations in nonplanar torsional geometries and steric effect. Bent of σ(O1-C6) bond orbital from the line of O-C centre decreases (1.0°) due to the presence of hydroxyl group close to it while O_1 NHO of σ(O_1-C_2) bond orbital show a large deviation of 2.2°. Hydroxyl group and carbonyl group increases the number of double bonds in coumarin moiety stabilizing the molecular π-system thereby distressing the π-electronic system of the neighbouring phenyl ring, partly destroying its aromaticity showing less stabilization energies 2.55, 2.46 kcal/mol for σC4-C19→σ*C19-C20, σ*C19-C24 interactions, respectively. Thus increased resonance stability and conjugation of lone pair interactions πC19-C20→π*C21-C22, πC23-C24→π*C21-C22 stabilize the entire system with energies 19.35 and 20.84 kcal/mol leading to strong delocalization energies -0.26700 and -0.26716, respectively. Same trend is shadowed over the entire part accompanied by deviations in bond length and bond angles of ring A. Hyperconjugative interactions associated with hybrid orbitals O15-H16 and O17-H18 due to $sp^{3.68}$ hybrid overlap on O15 and with $sp^{2.77}$ hybrid on O_{17}, respectively. Weak electrostatic O-H…O intra-molecular hydrogen bonding LP_1O1→σ*O17-H18, LP_1O17→σ*O15-H16 gives the measure which is very significant in the enrichment of the biological activity of this compound [22,23,24]. Inter-molecular O-H...O hydrogen bonding takes place between the solvent water molecule, and ring oxygen, hydroxyl groups of coumarin ring system and the solvent acts as hydrogen bond acceptor resulting strong inter molecular interactions LP_2O30→σ*(O17-H18) follows with stabilization energy 13.10 kcal/mol is confirmed. NHO mixing coefficients show slightly increased p-character leading to weak interactions between ring oxygen lone pair and solvent hydrogen atom LP_1O1 ($sp^{66.56}$)→σ*O30-H31 ($sp^{74.46}$) having less stabilization energy 0.15 kcal/mol also revealed. Table 1 shows second order perturbation analysis of Fock matrix using NBO basis of DHPC.

Carbon NHO of σ has 65.07% p character ($SP^{1.86}$) bent away from the line of C_3-C_4 centre by 2.7° due to steric repulsion effect around the centre. While orienting to coplanar, lower bending effect ensues at coumarin moiety junction C_4-C_{19} (1.3°) but carbon NHOs of bonds C_{21}-C_{22} and C_{23}-C_{24} constituting phenyl ring attached to coumarin ring shows deviation from the line of nuclear centre by (90.0°). Slight bending of σ(C_7-C_8) bond is minimized at an intermediate angle (104°) due to vicinal bonded oxygen atoms around these centre, accordingly bond σ(C_6-C_7) (3.7º) significantly bent away from the line of nuclei centre as a result of lying in the strong charge transfer path towards electron rich oxygen atoms O_1, O_{15} and O_{17}. In table 2 the bending angles of different bonds expressed as angle of deviation from the direction of the line joining the two nuclei centre.

Table 1. Second order perturbation analysis of Fock matrix using NBO basis.

Donor (i)	ED (i) (e)	Acceptor (j)	ED (j) (e)	E(2)[a] (kcal/ mol)	E(j) – E(i)[b] (a.u)	F(i,j)[c] (a.u)
within unit 1						
LP_1O1	1.96	σ*C2-C3	0.05	4.39	1.02	0.06
LP_1O1	1.96	σ*C5-C6	0.03	5.74	1.09	0.07
LP_1O1	1.96	σ*C6-C7	0.03	1.44	1.15	0.03
LP_1O1	1.96	σ*C2-O11	0.01	2.39	1.17	0.04
LP_1O1	1.96	σ*O17-H18	0.03	0.53	1.03	0.02
LP_2O1	1.75	π*C2-O11	0.31	34.55	0.35	0.10
LP_2O1	1.75	π*C5-C6	0.49	39.28	0.25	0.09
LP_2O11	1.83	σ*O1-C2	0.11	35.82	0.57	0.12
LP_2O11	1.83	σ*O1-C6	0.03	0.50	0.59	0.01
LP_2O11	1.83	σ*C2-C3	0.05	15.12	0.73	0.09
LP_1O15	1.97	σ*C7-C8	0.03	5.08	1.14	0.06
LP_2O15	1.85	π*C7-C8	0.42	35.98	0.27	0.09
LP_1O17	1.96	σ*C6-C7	0.03	7.28	1.17	0.08
LP_1O17	1.96	σ*C7-C8	0.03	1.07	1.11	0.03
LP_1O17	1.96	σ*O15-H16	0.01	0.99	1.06	0.02
LP_2O17	1.87	π*C7-C8	0.42	31.61	0.27	0.09
πC3-C4	1.79	π*C2-O11	0.31	26.46	0.28	0.08
πC3-C4	1.79	π*C5-C6	0.49	19.58	0.18	0.05
πC5-C6	1.62	π*C3-C4	0.19	18.34	0.29	0.06
πC5-C6	1.62	π*C7-C8	0.42	24.99	0.22	0.06
πC7-C8	1.60	π*C5-C6	0.49	35.75	0.17	0.07
πC9-C10	1.73	π*C5-C6	0.49	29.13	0.16	0.06
πC9-C10	1.73	π*C7-C8	0.42	27.85	0.21	0.07
σO17-H18	1.98	σ*C7-C8	0.03	2.30	1.21	0.04
σO17-H18	1.98	π*C7-C8	0.42	12.38	0.63	0.08
σC4-C19	1.96	σ*C19-C20	0.02	2.55	1.23	0.05
σC4-C19	1.96	σ*C19-C24	0.02	2.46	1.21	0.04
πC19-C20	1.65	π*C21-C22	0.32	19.35	0.29	0.06
σC20-C21	1.97	σ*C21-C22	0.01	13.14	1.70	0.13
πC23-C24	1.66	π*C21-C22	0.32	20.84	0.29	0.06
πC21-C22	1.65	π*C19-C20	0.35	19.33	0.32	0.07
πC23-C24	1.66	π*C19-C20	0.35	15.03	0.32	0.06
from unit 1 to unit 2						
LP_1O1	1.96	σ*O30-H31	0.01	0.15	2.94	0.01
LP_1O1	1.96	σ*O30-H32	0.01	0.12	2.82	0.01
σO17-H18	1.98	σ*O30-H31	0.0	2.36	3.06	0.07
σO17-H18	1.98	σ*O30-H32	0.00	7.63	2.94	0.13
from unit 2 to unit 1						
LP_1O30	1.99	σ*O1-C6	0.03	0.88	0.72	0.02
LP_2O30	1.96	σ*O1-C6	0.03	1.96	0.87	0.03
LP_2O30	1.96	σ*O17-H18	0.04	13.10	1.02	0.10
σO30-H31	1.99	σ*O1-C6	0.03	1.67	1.04	0.03
within unit 2						
LP_2O30	1.96	σ*O30-H32	0.00	18.23	2.81	0.20
LP_2O30	1.96	σ*O30-H31	0.01	43.49	2.93	0.32
LP_1O30	1.99	σ*O30-H32	0.00	37.61	2.65	0.28
LP_1O30	1.99	σ*O_{30}-H_{31}	0.01	3.20	2.77	0.08
σO30-H32	1.99	σ*O30-H32	0.00	56.53	2.93	0.36

σO30-H32	1.99	σ*O30-H31	0.01	34.79	3.05	0.29
σO30-H31	1.99	σ*O30-H32	0.00	19.90	2.98	0.21
σO30-H31	1.99	σ*O30-H31	0.01	2.13	3.10	0.07

a-E(2) means energy of hyperconjugative interactions; b-Energy difference between donor and acceptor i and j NBO orbitals; c-F(i,j) is the Fock matrix element between i and j NBO orbitals.

Table 2. NHO directionality bond bending analysis

Bond A-B	Line of Centre		Hybrid 1			Hybrid 2		
	Θ	φ	θ	Φ	Dev	θ	φ	Dev
πC2-O11	87.4	111.3	2.3	314.7	89.6	3.2	306.4	89.5
σO1-C6	94.1	284.2	94.1	285.2	1	85.7	99.4	4.7
πC3-C4	92.5	285.8	4.3	273.6	88.3	1.7	273	89.2
σC3-C4	92.5	285.8	94.7	284.4	2.6	90	106.9	2.7
σC4-C19	90.5	346.6	90.7	345.3	1.3	89.8	167.8	1.2
σC6-C7	92.1	219.5	-	-	-	87.5	43.2	3.7
σC7-C8	95.1	281.4	94.6	280.3	1.3	84.5	104.1	2.7
σC7-O17	87.5	164.6	87.4	160.7	3.9	92.6	346.1	1.5

3.3 FRONTIER ORBITAL ANALYSIS

Molecular orbital plots of the frontier orbitals for the ground state of DHPC molecule including the HOMO, LUMO, LUMO+1, LUMO+2 are shown in figure 2. In DHPC, HOMO and HOMO-1 are located on oxygen atoms of both hydroxyl and carbonyl group while HOMO-2 is localized on phenyl ring B. LUMO populates on bonded carbon atoms (C_8-O_{15}, C_6-O_1, C_5-C_4) and carbonyl group.

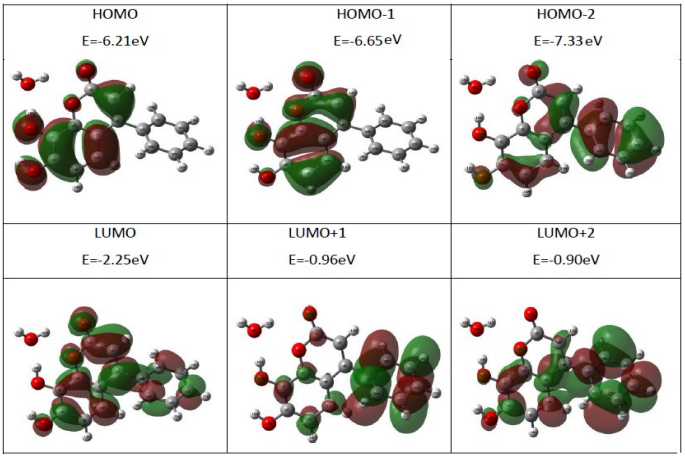

Figure 2. HOMO-LUMO Plot of DHPC

However, in LUMO+1 and LUMO+2 minor population is around the hydroxyl group and majority populates around the carbon atoms in ring C and ring B. Energy values of LUMO, HOMO and their energy gap reflect the chemical activity of the molecule. In addition, Lower HOMO-LUMO energy gap shows the possibility of intramolecular charge transfer analysis and confirms the bioactivity of the molecule [25]. Frontier orbital energy gap (E_{HOMO}–E_{LUMO}) is found to be -3.96 eV that is a critical parameter in determining charge transfer properties and bioactive efficiency [26]. Energy gap values of (HOMO-1)-(LUMO+1) and (HOMO-2)-(LUMO+2) are -5.68 eV and -6.44 eV, respectively leading the title compound to reflect its chemical stability and bioactivity. Electro negativity, chemical hardness and electrophilicity index values are correspondingly -4.23, 1.98 and 0.50 eV in gas phase.

3.4 ELECTRONIC SPECTRAL ANALYSIS

Strong UV absorption around 300 nm due to coumarin-characteristic chromophore has been reported [27] and spectra of 7-oxygenated coumarin show strong absorption bands at 315-330 nm with weak peaks or shoulders at 240-255nm [27]. Increased electron drift from electron donating and electron withdrawing groups through π-bond to ring B slightly shifts show shoulder primary band at 336, 334 and 334 nm for methanol, DMSO and ethanol, respectively.

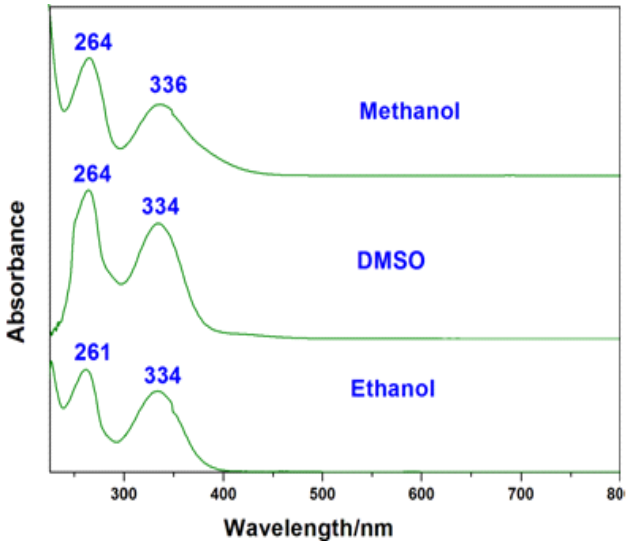

Figure 3. UV-Vis Spectra of DHPC

Double bond carbonyl chromophore show weak n→π* transition is shifted to 200-215 nm and intense electronic transition shows secondary band at 264, 264 nm and 261nm for methanol, DMSO and ethanol, respectively are assigned to *n*→π* transition for coumarin moiety. Electronic transitions from HOMO→LUMO having ≈

90% contribution calculated theoretically at 258, 254 and 254 nm for methanol, ethanol and DMSO, respectively is blue shifted from the experimental data about ≈ 10 nm. Theoretically calculated intense electronic transition for methanol, DMSO and ethanol are at 341, 343 nm and 343nm with an oscillator strength f = 0.1454, 0.1363 and 0.1299, respectively. Experimental peaks for various solvents such as methanol, DMSO and ethanol are shown in figure 3. Calculated excitation energies, absorbance and oscillator strength (f) for title molecule compared are tabulated in Table 3.

Table 3. Calculated excitation energies, absorbance and oscillator strength (*f*) of DHPC

Wave length(nm)		Energy (eV)	Osc.Strength (*f*)	Symmetry	Major contributes
Exp.	Cal.				
Solvent: Methanol					
336	341	2.92	0.14	Singlet-A	HOMO→LUMO (96%)
	315	3.17	0.17	Singlet-A	H-1→LUMO (84%)
	289	3.45	0.21	Singlet-A	H-2→LUMO (95%)
	280	3.56	0.01	Singlet-A	H-3→LUMO (97%)
264	258	3.86	0.01	Singlet-A	H-4→LUMO (93%)
	252	3.95	0.07	Singlet-A	HOMO→L+1 (68%)
Solvent :DMSO					
334	343	2.90	0.13	Singlet-A	H→L (96%)
	314	3.17	0.17	Singlet-A	H-1→LUMO (84%)
	291	3.43	0.21	Singlet-A	H-2→LUMO (96%)
	283	3.53	0.01	Singlet-A	H-3→LUMO (97%)
264	254	3.93	0.00	Singlet-A	H-4→LUMO (90%)
	251	3.97	0.09	Singlet-A	H-1→L+2 (81%)
Solvent : Ethanol					
334	343	3.61	0.12	Singlet-A	H→L (95%)
	314	3.94	0.17	Singlet-A	H-1→LUMO (83%)
	291	4.26	0.20	Singlet-A	H-2→LUMO (95%)
	282	4.38	0.00	Singlet-A	H-3→LUMO (97%)
261	254	4.86	0.00	Singlet-A	H-4→LUMO (91%)
	251	4.92	0.08	Singlet-A	HOMO→L+1 (67%)

IV. CONCLUSION

A complete structural, vibrational and electronic, studies of DHPC that have been carried out with spectroscopic techniques along with DFT method. NBO calculation agrees satisfactorily with the experimental interpretations confirming inter and intra-molecular hydrogen bonding interactions. HOMO-LUMO energies and their orbital energy gaps are calculated using B3LYP/6-311++G(d,p) method explaining the ultimate charge transfer interface within the molecule. Experimental UV absorption spectra measured in different solvents show intense broad and wide absorption bands and their peak positions are sensitive to solvent polarity.

V. REFERENCES

[1]. Mariusz Tasior et al. J. Org. Chem. 79(18) (2014) 8723.

[2]. Rashid Nazir, Anton J.Stasyuk, Daniel T.Gryko J.Org.Chem. 81(22) (2016) 11104.

[3]. J.B Hudson, E.A Graham, L Harris, M.J Ashwood-Smith J. Photochem Photobiol. 57(3) (1993) 491

[4]. Kimura Y, Okuda H, Journal of Natural Products (1997) 249-251.

[5]. Bubols G.B et al. Mini-Reviews in Medicinal Chemistry. 13(3) 318 (2013).

[6]. Venugopala K.N, Rashmi V, Odhav B BioMed Research International 14 (2013).

[7]. Donna L.Romero, Peter R. Manninen, Fusen Han, Arthur G. Romero J. Org. Chem. 64(13) 4980 (1999).

[8]. Zhao H, Neamati N, Hong H J. Med. Chem. 40 (1997) 242.

[9]. J.B Veselinović, J.S Matejić, A.M Veselinović , D SokoloviC Biologica Nyssana. 7 (2) (2016) 167.

[10]. T Adfa M,Itoh, Y Hattori, M Koketsu Biol. Pharm. Bull. 35(6) (2012) 963.

[11]. P.C. Hariharan, J.A. Pople Theoretica Chimica Acta.28 213-222 (1973).

[12]. R. Krishnan, J.S. Binkley, R. Seeger, J.A.Pople J. Chem. Phys.72 650-654 (1980).

[13]. A.D. Becke J. Chem. Phys. 98 5648-5652 (1993).

[14]. A.D. Becke Phys. Rev. A.38 3098-3100 (1988).

[15]. C.Lee, W.Yang, R.G. Parr Phys. Rev. B 37 785-789 (1988).

[16]. M.J.Frisch, G.W.Trucks, H.B.Schlegel, G.E. Scuseria, M.A. Robb, J.R.Cheeseman, G.Scalmani, V.Barone, B. Mennucci, G.A.Petersson, H.Nakatsuji, M.Caricato, X. Li, H.P.Hratchian, A.F.Izmaylov, J.Bloino, G.Zheng, J.L.Sonnenberg, M.Hada, M.Ehara, K.Toyota,

R.Fukuda, J.Hasegawa, M.Ishida, T.Nakajima, Y. Honda, O.Kitao, H. Nakai, T.Vreven, J.A.Montgomery Jr., J.E. Peralta, F.Ogliaro, M.Bearpark, J.J. Heyd, E. Brothers, K.N. Kudin, V.N. Staroverov, T. Keith, R. Kobayashi, J. Normand, K.Raghavachari, A. Rendell, J.C.Burant, S.S.Iyengar, J.Tomasi, M. Cossi, N. Rega, J.M. Millam, M. Klene, J.E. Knox, J.B. Cross, V. Bakken, C. Adamo, J. Jaramillo, R. Gomperts, R.E. Stratmann, O.Yazyev, A.J.Austin, R.Cammi, C.Pomelli, J.W.Ochterski, R. L.Martin, K. Morokuma, V.G. Zakrzewski, G.A.Voth, P. Salvador, J.J. Dannenberg, S. Dapprich, A.D. Daniels, O.Farkas J.B. Foresman, J.V. Ortiz, J. Cioslowski, D.J Fox, Gaussian 09, Revision C.02, Gaussian Inc.: Wallingford, CT.USA, (2009).

[17]. E.D. Glendening, A.E. Reed, J.E. Carpenter, F. Weinhold, "NBO 3.1", Theoretical Chemistry Institute and Department of Chemistry, University of Wisconsin, Madison, Wisconsin (1998).

[18]. W. Kohn, L.J. Sham Phys. Rev. A.140 A1133-1138 (1965).

[19]. R.G.Parr, W.Yang Density-Functional Theory of Atoms and Molecules, first edition, (London: Oxford University Press) (1994).

[20]. J.F. Himton, P. Pulay J. Amer. Chem. Soc. 112 8251-8260 (1990).

[21]. Kiran K. Pujar, Anilkumar G. N, Manohar V. Kulkarni, Crystal Structure Theory and Applications (2013) 88-92.

[22]. Jeffrey, A.George, An introduction to hydrogen bonding, Oxford University Press (1997).

[23]. Pauling L, The nature of the chemical bond. Cornell University Press, New York (1960).

[24]. P.J.A. Ribeiro-Claro, M.G.B. Drew, V. Felix, Chem. Phy. Lett. 356 (2002) 318-325.

[25]. K. Fukui, Science 218 (1982) 747–754.

[26]. M. Kurt, P. Chinna Babu, N. Sundaraganesan, M. Cinar, M. Karabacak, Spectrochim. Acta Part A 79 (2011) 1162–1170.

[27]. J Mohan Organic Spectroscopy Principles and Applications (New Delhi: Narosa Publishing House) (2009).